IAF-01-J.1.04

HIGH PRECISION ATOM INTERFEROMETRY IN SPACE : THE HYPER PROJECT

G. Bagnasco[1], R. Bingham[2], C. Bordé[3], P. Bouyer[4], M. Caldwell[2], A. Clairon[5], K. Danzmann[6], N. Dimarcq[7], W. Ertmer[8], L. Gerlach[1], J. Helmcke[9], C. Jentsch[8], B. Kent[2], C. Lämmerzhal[10], A. Landragin[7], M. Novara[1], I. Percival[11], E.M. Rasel[8], R. Reinhard[1], C. Salomon[12], M. Sanford[2], W. Schleich[13], P. Teyssandier[14] P. Tourrenc[15], S. Vitale[16], P. Wolf[5]

(1) ESTEC, ESA, The Netherlands
(2) Rutherford Appleton Laboratory , United Kingdom
(3) Laboratoire de Physique des lasers, France
(4) Laboratoire Charles Fabry, France
(5) Laboratoire Primaire du Temps et des Fréquences, France
(6) Institut für Atom und Molekülphysik, Germany
(7) Laboratoire de l'Horloge Atomique, France
(8) Institut für Quantenoptik, Germany
(9) Physikalisch-Technische Bundesanstalt, Germany
(10) Universität Düsseldorf, Germany
(11) Queen Mary and Westfield College, United Kingdom
(12) Laboratoire Kastler-Brossel, France
(13) Universität Ulm, Germany
(14) DANOF Observatoire de Paris, France
(15) Université Pierre et Marie Curie, France
(16) University of Trento, Italy

52ND INTERNATIONAL ASTRONAUTICAL CONGRESS
1-5 OCT 2001/TOULOUSE, FRANCE

HIGH PRECISION ATOM INTERFEROMETRY IN SPACE : THE HYPER PROJECT

G. Bagnasco[(1)], R. Bingham[(2)], C. Bordé[(3)], P. Bouyer[(4)], M. Caldwell[(2)], A. Clairon[(5)], K. Danzmann[(6)], N. Dimarcq[(7)], W. Ertmer[(8)], L. Gerlach[(1)], J. Helmcke[(9)], C. Jentsch[(8)], B. Kent[(2)], C. Lämmerzhal[(10)], A. Landragin[(7)], M. Novara[(1)], I. Percival[(11)], E.M. Rasel[(8)], R. Reinhard[(1)], C. Salomon[(12)], M. Sanford[(2)], W. Schleich[(13)], P. Teyssandier[(14)] P. Tourrenc[(15)], S. Vitale[(16)], P. Wolf[(5)]

(1) ESTEC, ESA, The Netherlands
(2) Rutherford Appleton Laboratory , United Kingdom
(3) Laboratoire de Physique des lasers, France
(4) Laboratoire Charles Fabry, France
(5) Laboratoire Primaire du Temps et des Fréquences, France
(6) Institut für Atom und Molekülphysik, Germany
(7) Laboratoire de l'Horloge Atomique, France
(8) Institut für Quantenoptik, Germany
(9) Physikalisch-Technische Bundesanstalt, Germany
(10) Universität Düsseldorf, Germany
(11) Queen Mary and Westfield College, United Kingdom
(12) Laboratoire Kastler-Brossel, France
(13) Universität Ulm, Germany
(14) DANOF Observatoire de Paris, France
(15) Université Pierre et Marie Curie, France
(16) University of Trento, Italy

We present the core technique of the HYPER mission : the matter wave based inertial sensors. We will first briefly introduce the basics of matter wave interferometry by focusing and light pulse interferometers that will be used on HYPER. After reviewing different applications of inertial sensors, we will focus on the applications of Atomic Sagnac Units (ASU) to measure the Lense & Thirring effect around the earth. We will conclude with possible other mission goals such as tests of QED.

INTRODUCTION

Inertial Sensors are useful device in both science and industry. Higher precision sensors could find practical scientific applications in the areas of general relativity[1], geodesy and geology. Important applications of such devices occur also in the field of navigation, surveying and analysis of structures.

Matter-wave interferometry has recently shown its potential to be an extremely sensitive probe for inertial forces[2]. For example, neutron interferometers have been used to measure the rotation of the earth[3] and the acceleration due to gravity[4]. More recently, atom interference techniques have been used in proof-of-principle work to measure rotations[5] and accelerations[6].

ATOM INTERFEROMETER-BASED INERTIAL SENSORS : BASIC PRINCIPLE

We present here a summary of recent work with light-pulse interferometer-based inertial sensors. We first outline the general principles of operation of light-pulse interferometers. This atomic state interferometer[7] uses two-photon velocity selective Raman transitions[8,9] to manipulate atoms while keeping them in long-lived ground states. In these interferometers, the atomic internal states plays the role of polarization in photonic optics.

Principle of a light pulse matter-wave interferometer

Light-pulse interferometers work on the principle that when an atom absorbs or emits a photon momentum must be conserved between the atom and the light field. Consequently, an atom which emits (absorbs) a photon of momentum[i] $\hbar\mathbf{k}$ will receive a momentum impulse of $\delta\mathbf{p} = -\hbar\mathbf{k}(+\hbar\mathbf{k})$. When a resonant traveling wave is used to excite the atom, the internal state of the atom becomes correlated with its momentum: an atom is in its ground state $|1\rangle$ with momentum $\mathbf{p}$ (labeled $|1,\mathbf{p}\rangle$) is coupled to an excited state $|2\rangle$ of momentum $\mathbf{p}+\hbar\mathbf{k}$ ($|2,\mathbf{p}+\hbar\mathbf{k}\rangle$)[7]. This is analogous to, for example, a polarizing beam splitter (PBS) in optics, where each outpout port of the PBS (i.e. the photon momentum) is correlated to the laser polarization (i.e. the photon state). In the optical case, a precise control of the input beam polarization allows for controlling the balance between the output ports. In the case of atoms, a precise control of the light-pulse duration plays the role of the polarization control, allowing a complete transfer from one state (for example $|1,\mathbf{p}\rangle$) to the other ($|2,\mathbf{p}+\hbar\mathbf{k}\rangle$) in the case of a π pulse and a 50/50 splitting between the 2 states in the case of a $\pi/2$ pulse (half the duration of a π pulse).

We use a $\pi/2-\pi-\pi/2$ pulse sequence[10] to coherently divide, deflect and finally recombine an atomic wavepacket[ii]. The first $\pi/2$ pulse excites an atom initially in the $|1,\mathbf{p}\rangle$ state into a coherent superposition of states $|1,\mathbf{p}\rangle$ and $|2,\mathbf{p}+\hbar\mathbf{k}\rangle$. If state $|2\rangle$ is stable against spontaneous decay, the two wavepackets will drift apart by a distance $\hbar\mathbf{k}T/m$ in time T. Each wavepacket is redirected by a π pulse which induces the transitions $|1,\mathbf{p}\rangle \rightarrow |2,\mathbf{p}+\hbar\mathbf{k}\rangle$ and $|2,\mathbf{p}+\hbar\mathbf{k}\rangle \rightarrow |1,\mathbf{p}\rangle$. After another interval T the wavepackets once again overlap. A final $\pi/2$ pulse causes the two wavepackets to interfere. The interference is detected, for example, by measuring the number of atoms in the $|2\rangle$ state.

We obtain large wavepacket separation by using laser cooled atoms and velocity sensitive stimulated Raman transitions[8] to drive the transitions. it gives large recoil kicks $\hbar\mathbf{k}/m$ in transition between ground-state hyperfine levels.

Applications to inertial force sensors

Inertial forces manifest themselves by changing the relative phase of the de Broglie matter waves with respect to the phase of the driving light field, which is anchored to the local reference frame. The physical manifestation of the phase shift is a change in the number of atoms in, for example, the state $|2\rangle$, after the interferometer pulse sequence as described above.

If the 3 light pulses of the pulse sequence are only separated in time, and not separated in space (i.e. if the velocity of the atoms is parallel to the laser beams), the interferome-

---

[i] Even though photon has no mass, it carries momentum which is proportional to the radiation frequency. This property, foreseen by A. Einstein, was already used in 1933 by Frisch to explain the direction of the tail of the comets.

[ii] A wavepacket is the quantum mechanics equivalent of a partially coherent light vibration. The wavepacket denotes the spatial extension over which all monochromatic "atomic" vibrations will interfere constructively and the size of this wavepacket can therefore be seen as the coherent length of the atomic source. Colder atoms lead to longer coherence length. For example, atoms cooled at 1 μK have a coherence length of about 1 μm.

ter is in a gravimeter or accelerometer configuration[11]. In a uniformely accelerating frame with the atoms, the frequency of the driving laser changes linearly with time at the rate of $-\mathbf{k}_{\text{eff}} \cdot \mathbf{a}t$ because of the Doppler effect. The phase shift arises from the interaction between the light and the atoms[12] and can be written

$$\Delta\phi \equiv \phi_1(t_1) + \phi_2(t_2) + \phi_3(t_3)$$

where $\phi_i(t_i) = \int_{t_0}^{t_i} \delta(t)dt$ is the phase of light pulse I at time t_1 relative to the atoms (δ is the laser detuning : the difference between the chirped frequency of the laser vibration and the atomic transition frequency[iii]). If the laser beams are vertical, the gravitationally induced chirp can be written:

$$\Delta\phi \equiv -\mathbf{k}_{\text{eff}} \cdot \mathbf{g}T^2$$

It should be noted that this phase shift does not depend on the atomic initial velocity or on the mass of the particle. A first experiment demonstrated a sensitivity of 3 parts in 10^8 after integrating for 2000 sec[11]. More recently, accuracy comparable to the precision obtained by measuring g with a falling corner cube under the best seismic conditions has been achieved[13].

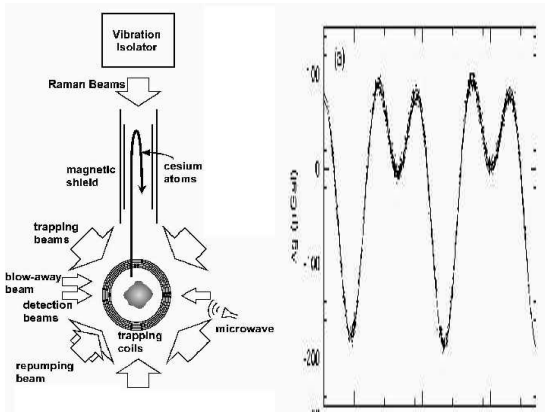

Principle of the atom-fountain-based atom gravimeter achieved in S. Chu (Nobel 1998) group at Stanford. Left shows a two days recording showing the variation of gravity. The accuracy allowed to resolve ocean loading effects.

Gravimetric survey using gravimeters does not yield the spatial resolution and the accuracy that is typically needed. The major reasons for the shortfall are associated with spurious acceleration from the platform the sensor is mounted on. Altitude uncertainties can also lead to errors in the reference gravity field. In principle, such problems disappear if the gravity field gradient is measured rather than the gravity field itself. The use of two independant atom-interferometer based accelerometers, as described above, can provide gravity gradient measurement by comparing acceleration measurements at two locations separated by a fixed distance. In this geometry, the light pulses propagate along a direction passing through two spatially separated ensembles of laser cooled atoms. Following a three-pulse interferometer sequence, the number of atoms making the transition at both regions is recorded, and the gravitationally induced phase shifts are extracted. The change of the projection of along the direction of the beams may then be derived from the difference of the two phase shifts and the distance between the sources. The design sensitivity of $\sim 10^{-7}\ \text{s}^{-2}/\sqrt{\text{Hz}}$ competes fa-

[iii] The atomic transition frequency ω_0 represents the energy $\hbar\omega_0$ that one photon from the laser has to communicate to the atom to allow the change of electronic state. Since the photon energy is related to the laser wavelength and hence its frequency, the atomic transition can be driven by laser light only if the laser frequency is equal to the atomic transition.

vorably with the existing instruments.

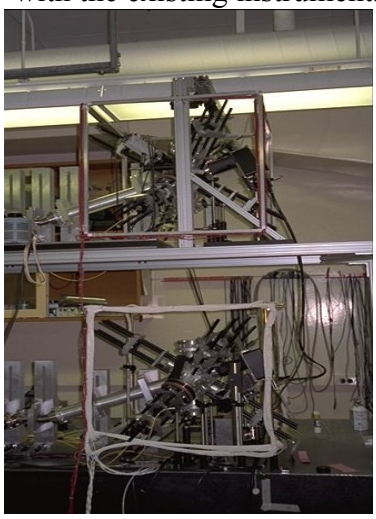

Photo of the atomic gradiometer built in Yale University. One clearly sees 2 cold atom sources (Magneto-Optical Traps).

If the laser beams are now separated in space (i.e. if the atomic velocity is perpendicular to the direction of the laser beams), the interferometer which is formed is in a Mach-Zenhder configuration. In this case, the interferometer is sensitive to rotations, as in the Sagnac geometry[14]. For a Sagnac loop enclosing area **A**, a rotation **Ω** produces a shift:

$$\Delta\phi = \frac{4\pi}{\lambda v}\boldsymbol{\Omega}\cdot\mathbf{A}$$

where λ is the particle wavelength and v its velocity[iv].

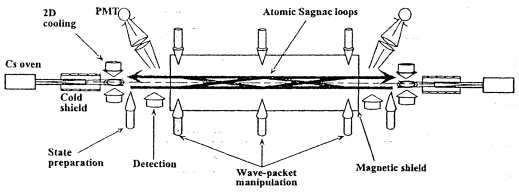

Schematic of the atomic Sagnac interferometer at Yale [27]. The figure shows an atomic Sagnac interferometer based on thermal atoms. Two atomic beams are emerging from two ovens on the left and right side and counter propagate to each other. The atomic waves are coherently split by the same laser beams and independently detected by observing the fluorescence. Due to highly symmetric set-up many disturbances due to the environment could be ruled out. This Sagnac interferometer is almost shot-noise limited.

Consequently, the inherent sensitivity of a matter-wave gyroscope exceeds that of a photon-based system by a factor of $mc^2/\hbar\omega \sim 10^{11}$ (m is the particle mass, ω the photon frequency)[v]. Although optical gyroscopes have higher particle fluxes and larger enclosed areas, atom-based systems still outperform optical systems by several orders of magnitude.

The minimal rotation rate which can be resolved is in the best case limited by the shot-noise. In that case the noise amplitude of the atomic beam scales with the square root of the averaged flux (i.e. the square root of the standard deviation of the flux from the mean) and, thus, a high atomic flux is essential. For 10^{10} atoms/s the white shot noise would be e.g. 10^5 atoms/s at a 1Hz frequency bandwidth.

$$\Delta\Phi^{atoms}_{Saganc,\min} = 2\pi\,\frac{2\,m_{at}}{h}\,A\cdot\frac{\Delta N}{N}$$

[iv] The atomic wavelength, or de Broglie wavelength, has been introduced by Louis de Broglie in 1918. It denotes the quantum behavior of matter via its wave-particule duality, namely the fact that matter can behave like waves (with the "matter" or "atomic" radiation having a frequency proportional to its velocity) and vice versa (light radiation gives rise to photons, pressure or sonic vibrations give rise to phonons).

[v] This ratio is simply the ratio of relativistic energies mc^2 for the atoms and $\hbar\omega$ for the light.

In the case of the caesium Sagnac interferometer described above the resolution $\frac{\partial\Phi}{\partial\Omega}$ is about 10^{-5} rad/s for an enclosed surface of 0.2 cm^2. In the shot noise limit the sensitivity is $2\cdot10^{-10}$ rad/s$\cdot\sqrt{Hz}$ for a signal amplitude of 10^{10} atoms/s.

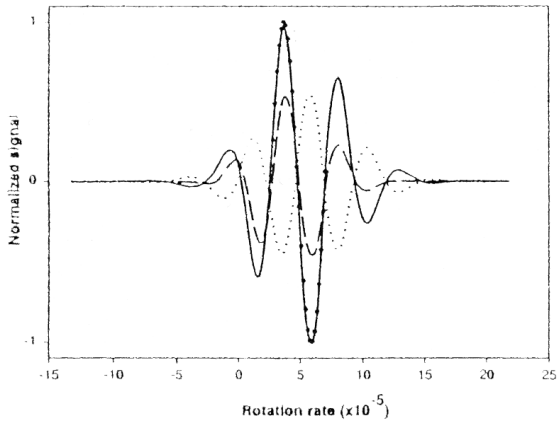

The individual signals at the output of the two counter-propagating atom interferometers (doted and broken lines) and the difference of both signals. Unlike phase shifts due to accellerations, the Sagnac phases measured by the two counter-propagating interferometer have opposite sign:

$$S_{I.AI} \sim \cos(\Phi_L + \Phi_{Sag} + \Phi_{Acc})$$
$$S_{II.AI} \sim \cos(\Phi_L - \Phi_{Sag} + \Phi_{Acc})$$

Further increases of this impressive sensitivity can be achieved by changing the atomic flux and the enclosed area. While the atomic flux is already considerable, the enclosed surface is rather small compared to the overall length of the apparatus of 2 m. Caesium is one of the best choices, because it has a high vapour pressure even at room temperatures and a rather large atomic mass (133 u). Thus, atomic beams with a high atomic flux and slow velocities (a couple of 100 m/s) can be realised. In addition, caesium can be manipulated easily with laser light generated by solid state lasers (laser diodes). The atomic mass is however less important as one might conclude from the preceding discussion. Nevertheless, the achievable surface in an atom interferometer depends also on the atomic mass. The size of the surface is determined by the ratio of the atomic beam velocity v_L to the velocity v_T of both atomic waves relative to each other due to the beam splitting process. The recoil velocity transferred to the atom by the atom light interaction scales inversely with the atomic mass for a given photon momentum $\hbar k$, while the velocity of the atomic beam scales for a given temperature T of the atomic ensemble with the square root of the mass.

$$A = L^2 \cdot \frac{v_T}{v_L} \propto \frac{1}{\sqrt{m_{at}}}$$

$$v_T = \frac{\hbar k}{m_{at}} \propto \sqrt{\frac{2k_B T}{m_{at}}}$$

The highest potential for further improvements of an atomic Sagnac interferometer relies therefore on the increase of the enclosed surface: Using cold atoms with a lower velocity, one can achieve a ratio of v_T/v_L close to unity. The improvements with HYPER will follow precisely this philosophy keeping the atomic flux at the same time as high as possible. Presently first prototypes based on atomic fountains of laser cooled atoms are under construction in a joint project of LPTF , IOTA and LHA in Paris as well as at the IQO in Hanover.

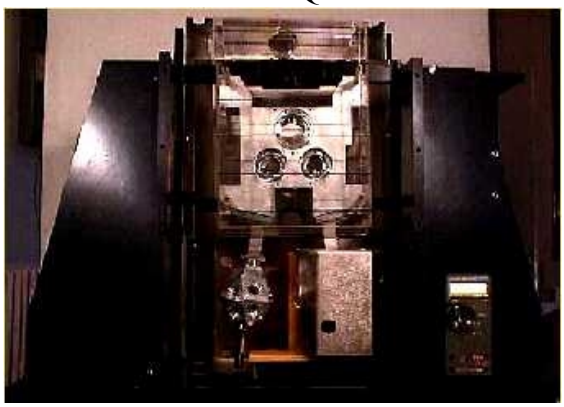

Picture of the cold atom inertial base (gyroscope and accelerometer) in fabrication in Observatoire de Paris (France)

LATITUDINAL MAPPING OF THE GRAVITOMAGNETIC EFFECT WITH HYPER

The high sensitivity of atomic Sagnac interferometer for rotation rates will enable HYPER to measure even the latitudinal structure of the gravitomagnetic or Lense-Thirring effect while the satellite orbits around the Earth. In terms of atom interferometry the rotation Ω_{LT} induced by the gravitomagnetic effect of the spinning Earth induces an additional Sagnac phase $\Delta\Phi_{Sagnac}$:

$$\Delta\Phi_{Sagnac} = 2\pi \frac{2\, m_{at}}{h} \vec{A}\cdot\vec{\Omega}_{LT}$$

where

$$\vec{\Omega}_{LT}(r) = \frac{GI}{c^2}\frac{3\,(\vec{\omega}\cdot\vec{r})\vec{r} - \vec{\omega}\, r^2}{r^5}$$

is the Lense & Thirring effect.

Entering the interferometer the matter wave is coherently split by the atom-light interaction acting as beam splitter mechanism and travels along two spatially separated paths until it is recombined. The Earth's drag Ω_{LT} bends these two distinct trajectories followed by the matter wave, while the orientation of the atomic beam splitter which serves as reference remains fixed at an inertial system, a far distant guide star pursued by a high-performance telescope.

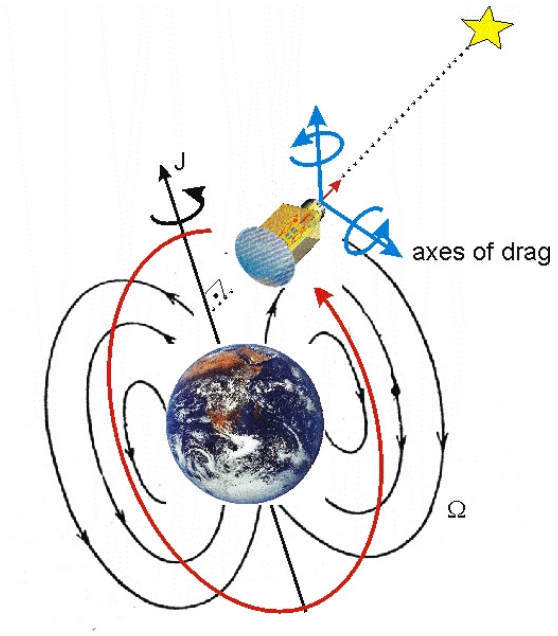

Schematic of the measurement of the Lense-Thirring effect. The black lines visualise the vector field of the Earth's drag Ω_{LT}. The satellite's orbit is marked red. The sensitive axes (blue) of the two ASUs are perpendicular to the pointing of the telescope. The direction of the Earth's drag varies over the course of the orbit showing the same structure as the field of a magnetic dipole. Due to this formal similarity the Lense-Thirring effect is also called gravitomagnetic effect. It has to be pointed out that there is no connection to electromagnetism.

In a Sun-synchronous, circular orbit at 700 km altitude, HYPER will detect how the direction of the Earth's drag varies over the course of the near-polar orbit as a function of the latitudinal position ϑ:

$$\begin{pmatrix}\Omega_x\\ \Omega_y\end{pmatrix} \propto \frac{3}{2}\begin{pmatrix}\sin 2\vartheta\\ \cos 2\vartheta - \frac{1}{3}\end{pmatrix}$$

with $\vec{J}\,\|\,\vec{e}_y$, $\vartheta \equiv \arccos(\vec{r}\cdot\vec{e}_x)$ the coordinate system, spanned by e_x and e_y, defines the orbital plane.

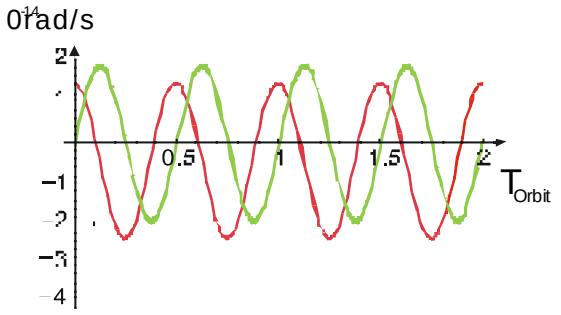

The rotation Ω_{LT} due to Earth's gravitomagnetism as sensed by the two orthogonal ASUs (red and green) in the orbit around the Earth. The satellite completes one orbit in the time T_{Orbit}.
Rotation rate at pole: $+1.25\_10^{-5}$ nrad/s
Rotation rate at equator: -2.5_10^{-5} nrad/s

The drag which the matter wave experiences is strongest over both Earth's poles. There, the matter wave will start to follow Earth's rotation. At the Earth's equator the drag has the opposite sign and half the amplitude as on the two poles. An intuitive explanation for the behaviour at the equator refers to the dependence of the Lense-Thirring effect on the relative distance: The matter wave experiences a stronger drag travelling along the trajectory closer to the Earth as on trajectory turned away from the Earth. The rotation sensed by the atoms has the opposite sign of the Earth's rotation as in the case of two interconnected gearwheels. The sign of the Sagnac phase shift is therefore reversed with respect to the shift over the two poles.

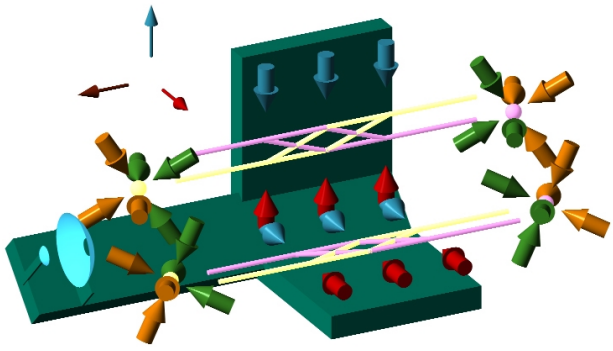

Baseline configuration of the ASUs in HYPER : The atomic Sagnac unit (ASU) is a device to measure rotations and accelerations with by interferometric means. For both kind of motions the device shows a highly directional sensitivity. In order to measure all accelerational and rotational vector components three ASUs would have to be used, arranged in orthogonal orientations. The objective of HYPER is to measure the Lense-Thirring effect, for this the rotations and accelerations in only two directions need to be measured. Hence, for HYPER, the complete payload will consist of only two orthogonal ASUs.

HYPER carries two atomic Sagnac interferometers, each of them is sensitive for rotations around one particular direction. The two units will measure the vector components of the gravitomagnetic rotation along the two axes perpendicular to the telescope pointing which is directed to a guide star. The drag variation written above describes the situation for a telescope pointing in the direction perpendicular to the orbital plane of the satellite. The orbit, however, changes its orientation over the coarse of a year which has to be compensated by a rotation of the satellite to track continuously the guide star. Consequently the pointing of the telescope is not always directed parallel to the normal of the orbital plane.

As discussed before, the rotation rate will alternate between the two poles and the equator resulting in a periodically changing signal with twice the frequency of the satellites revolution around the Earth. At the two poles the rotation rate reaches the maximum value of $-2.5 \cdot 10^{-14}$ rad/s, while on the equator the rotation rate changes its sign and becomes $1.25 \cdot 10^{-14}$ rad/s. The resolution of the atomic Sagnac units is about 10^{-12} rad/s for a drift time of about 3 s. Repeating this measurement all 3 seconds the ASU's will reach after 2 hours the level of 10^{-14} rad/s, in the course of one year the level of 10^{-16} rad/s, i.e. a hundredth of the expected effect.

CONCLUSION

We reviewed inertial sensors using atomic interferometry techniques which are expected to exhibit largely improved sensitivities compared to those relying on optical interferometry. Like atomic clocks, they must take benefit from the use of cold atoms. Previous experiments measuring the gravitational acceleration of Earth and its gradient (in an atomic fountain) or rotations (in a Sagnac interferometer) have been demonstrated to be very promising. Sensitivities better than 1 nrad.s^{-1}.$Hz^{-1/2}$ for rotation measurements and 10^{-9}g.$Hz^{-1/2}$ for gravity measurement have already been obtained. Gravity is the most fundamental impediment to take full advantage of the superior potential of cold atom physics. The sensitivity of matter-wave interferometers for rotations and accelerations increases with the measurement time and can therefore be dramatically enhanced by reducing the atomic velocity. Laser cooling can efficiently reduce the speed of the atoms but cannot circumvent the acceleration due to gravity. Measures to compensate for gravity with additional forces perturb unavoidably the sensor. On the ground the 1-g environment sets clear limitations for ultimate sensitivities.

HYPER-precision atom interferometry in space opens up entirely new possibilities for research in fundamental physics with unprecedented precision. The cold atom interferometers carried by HYPER will be accommodated in a drag-free spacecraft in a low-Earth, Sun-synchronous orbit. The primary scientific objectives of the HYPER mission are to test General Relativity by mapping (latitudinal) structure (magnitude and sign) of the Lense-Thirring effect, to determine the fine structure constant by measuring the ratio of Planck's constant to the atomic mass and to test the equivalence principle on individual atoms, a complement to other space tests of the equivalence principle using massive bodies (STEP, MICROSCOPE)

---

[1]W. Chow *et al.* Rev. Mod. Phys. **57**, 61 (1985).
[2]J.F. Clauser, Physica B **151**, 262 (1988)
[3]R. Colella, A. Overhauser, and S. Werner, Phys. Rev. Lett. **34**, 1472 (1975).
[4]S.A. Werner, J.L. Staudenmann, And R. Colella, Phys. Rev. Lett. **42**, 1103 (1979).
[5]F. Riehle *et al.,* Phys. Rev. Lett. **67**, 177 (1991).
[6]G. Stedman *et al.*, Phys. Rev. A **51**, 4944 (1995).
[7]C.J. Bordé, Phys. Lett. A **140**, 10 (1989).
[8]M. Kasevich et al., Phys. Rev. Lett. **66**, 2297 (1991).
[9]K. Moler, D.S. Weiss, M. Kasevich, and S. Chu, Phys. Rev. A **45**, 342 (1992)
[10] See for example: L. Allen, J.H. Eberly*: Optical Resonance and two level atoms*, Wiley, New York (1975)
[11]M. Kasevich and S. Chu, Appl. Phys. **67**, 177 (1991)
[12]For a detailed calculation see B. Young, M. Kasevich and S. Chu, *in Advances in Atomic and molecular Physics, Atom Interferometry*, edited by P. Berman (1996)
[13]A. Peters, K. Chung and S. Chu, private comm. (1996).
[14]M. Sagnac, Compt. Rend. Acad. Sci. **157**, 708 (1913).